Elliptical Flow Instability in a Conducting Fluid Triggered by an External Magnetic Field

Konrad Bajer*
Faculty of Physics, University of Warsaw, ul. Pasteura 7, 02-093 Warsaw, Poland

Krzysztof Mizerski†
Department of Magnetism, Institute of Geophysics, Polish Academy of Sciences, ul. Księcia Janusza 64, 01-452 Warsaw, Poland
(Received 16 July 2008; revised manuscript received 30 October 2010; published 6 March 2013)

We demonstrate that arbitrarily weak magnetic field may cause violent instability of an anticyclonic, recirculating flow with uniform mean angular velocity. This magnetohydrodynamic instability would trigger turbulence in the cores of vortices where neither centrifugal, exchange instability, nor magneto-rotational instability is effective. In the accretion disk vortices this can be an important mechanism of enhanced outward transport of angular momentum.

DOI: 10.1103/PhysRevLett.110.104503 PACS numbers: 47.20.Cq, 47.35.Tv, 95.30.Qd, 97.10.Gz

Externally imposed magnetic field is usually a factor that stabilizes the magnetohydrodynamic flows (e.g., the Taylor-Couette flow between solid cylinders [1,2]). A surprising counterexample is the magnetorotational instability (MRI) discovered by Velikhov [3] and then elucidated by Chandrasekhar [4] followed by Balbus and Hawley [5]. Since its discovery it has attracted great interest as a possible mechanism of turbulence enhancement in the accretion disks that may be responsible for the efficient transport of angular momentum inferred from observations [6]. Without magnetic field recirculating flows are subject to centrifugal (exchange) instability when angular momentum is outwardly decreasing [for power-law azimuthal velocity $u_\theta(r) \sim r^{n+1}$ it means $n < -2$], so Keplerian disks [$u_\theta(r) \sim r^{-1/2}$] are not affected. However, with the magnetic field present, no matter how weak, the class of unstable velocity profiles is much extended. The MRI acts in flows with outwardly decreasing angular velocity ($n < 0$) and those include the Keplerian profile but still exclude flows with linear profile [$u_\theta(r) \sim r^{+1}$], i.e., flows with *uniform* angular velocity (vorticity) which is approximately the case in the cores of vortices.

We demonstrate that a wide class of uniform vorticity flows, such as cores of anticyclonic vortices in a rotating frame, are also subject to a violent instability, provided they are nonaxisymmetric. This instability differs from the MRI. Unlike the MRI it affects the linear profile flows but, also unlike the MRI, depends on the elliptical deformation of streamlines. However, it has one important characteristics of the MRI. In the weak-field limit its onset and its growth rate are independent of the magnetic field strength, so even a seed field is a trigger of the powerful *flow instability*, namely, elliptical instability [7,8]. We show that the dominant elliptical instability modes (horizontal modes), which in anticyclonic vortices would otherwise be stable, are triggered by the magnetic field.

The physical situation we have described, i.e., elliptical vortex core with background rotation and axial magnetic field, is likely to occur in at least some types of accretion disks. Vertical field in a disk is believed to be a fairly common occurrence recently confirmed by observations [9]. Observed large scale asymmetries in the distribution of dust [10] are attributed to vortices generated, possibly, by the Rossby wave instability acting on the scale of the entire disk [11]. Earlier simulations suggested vortex generation by the disruptions of the zonal shear flow ("cat's eyes") [12]. When the zonal flow has outward-decreasing angular velocity, the emerging vortices, obviously, will be anticyclonic, so they will be affected by this instability. Numerical simulations indeed showed the evidence of such structures being unstable with respect to the vertically propagating perturbations [13].

Stability of elliptical flows is of great interest in the context of planetary interiors. For a comprehensive study of the effect of precession, see Refs. [14,15]. Those works were mainly concerned with the asymptotic analysis in the limit of small ellipticity (Ref. [15] also found the growth rates of the horizontal modes in their configuration).

In this Letter, motivated by the significance of the magnetic instabilities for the dynamics of accretion disks, we study the conditions under which the magnetic field triggers the instability in an elliptic vortex subject to background rotation. In Ref. [16], horizontal modes were computed numerically. Here we analytically derive the dispersion relation, provide a complete stability map in the parameter space, and highlight physical implications.

We write the equations of ideal magnetohydrodynamics in a frame of reference steadily rotating with angular velocity $\mathbf{\Omega} = \Omega \hat{\mathbf{e}}_z$,

$$\frac{\partial \mathbf{u}}{\partial t} + (\mathbf{u}\cdot\nabla)\mathbf{u} = -\rho^{-1}\nabla P - 2\mathbf{\Omega}\times\mathbf{u} + \rho^{-1}\mathbf{j}\times\mathbf{B}, \quad (1a)$$

$$\frac{\partial \mathbf{B}}{\partial t} + (\mathbf{u}\cdot\nabla)\mathbf{B} = (\mathbf{B}\cdot\nabla)\mathbf{u}, \quad (1b)$$

$$\nabla\cdot\mathbf{u} = 0, \quad \nabla\cdot\mathbf{B} = 0, \quad \mathbf{j} = \mu^{-1}\nabla\times\mathbf{B}, \quad (1c)$$

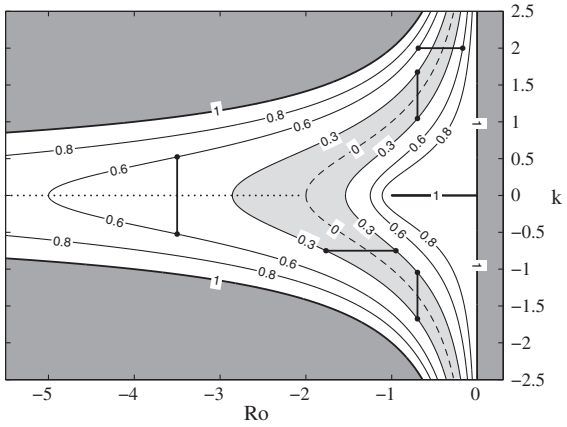

FIG. 1. Stability diagram of the HI modes in the (Ro, k) space. Level contours of $|\chi_+|$ are shown. Dark gray area and the interval ($k = 0$, $-1 \le \mathrm{Ro} \le 0$) mark the region where $|\chi_+| \ge 1$ (stable for all ϵ). The instability condition ($|\chi_+| < |\epsilon|$) is satisfied inside regions bordered by $|\chi_+| = |\epsilon|$ contours (light gray band is an example for $|\epsilon| = 0.3$). Maximum growth rate σ_m is marked with broken lines, dashed when $\mathrm{Ro} > -2$ ($\chi_+ = 0$ contour), and dotted when $\mathrm{Ro} \le -2$. Bars show how to read when the vortex of given ϵ is unstable. Vertical bars mark the ranges of unstable k for (Ro, $|\epsilon|$) = (-3.5, 0.6) (left) and (-0.7, 0.3) (right). Horizontal bars show ranges of unstable Ro for (k, $|\epsilon|$) = (2, 0.6) (upper) and (-0.75, 0.3) (lower).

where ρ is fluid density, μ its permeability and $P(\mathbf{x}, t)$ is the pressure field including the potential of the centrifugal force.

We consider linear stability of a vortical flow with elliptical streamlines [8] and with uniform magnetic field aligned with the axis of rotation,

$$\mathbf{U}_0 = \gamma[-(1+\epsilon)y, (1-\epsilon)x, 0], \qquad \mathbf{B}_0 = B_0\hat{\mathbf{e}}_z, \quad (2)$$

where $-1 < \epsilon < 1$ is a measure of eccentricity.

The characteristic scales of time, velocity, and length in this basic flow are given by

$$\gamma^{-1}, \qquad u_A = B_0(\rho\mu)^{-1/2}, \qquad u_A\gamma^{-1}, \quad (3)$$

where 2γ is the (uniform) relative vorticity and u_A is the Alfvén speed. The magnitude of the background rotation is characterised by the Rossby number,

$$\mathrm{Ro} = \gamma/\Omega. \quad (4)$$

When Ro is positive (negative) the vortex is called cyclonic (anticyclonic). The (nondimensional) angular frequency of the vortex is $\omega = (1-\epsilon^2)^{1/2}$ [17] (alternative scaling could be used instead with turnover time taken for a unit).

Linearizing the dimensionless form of (1) we obtain equations for infinitesimal perturbations $\mathbf{u}'$, $\mathbf{B}'$, P', These equations admit solutions in the form of inertial waves, also known as Kelvin modes (as in the rapid distortion theory [18–20]),

$$[\mathbf{u}', \mathbf{B}', P'] = [\mathbf{v}(t), \mathbf{b}(t), p(t)]e^{i\mathbf{k}(t)\cdot\mathbf{x}}, \quad (5)$$

The components in the (x, y) plane (called the "horizontal plane" although gravity is not taken into account in this problem) are decoupled from the vertical components. We shall now focus on a special class of disturbances, called *horizontal perturbations*, in which the vertical components identically vanish,

$$k_x = k_y = 0, \qquad b_z = v_z = 0, \qquad |\mathbf{k}| = k_z = k. \quad (6)$$

Then the amplitudes of the Kelvin modes satisfy the ordinary differential equations

$$\dot{\mathbf{v}} = -(\hat{A} + 2\mathrm{Ro}^{-1}\hat{O})\mathbf{v} + ik\mathbf{b}, \qquad \dot{\mathbf{b}} = \hat{A}\mathbf{b} + ik\mathbf{v}, \quad (7)$$

where $\hat{A}$ is the velocity gradient and $\hat{O}$ is the rotation matrix [16]. If we write the horizontal components as a single four-component vector, $\mathbf{s} = (v_x, v_y, b_x, b_y)$, then Eq. (7) can be written as $\dot{\mathbf{s}} = \hat{S}_0\mathbf{s}$. The matrix $\hat{S}_0$ has four eigenvalues,

$$\sigma_+^{\pm} = \pm(\epsilon^2 - \chi_+^2)^{1/2}, \quad \sigma_-^{\pm} = \pm(\epsilon^2 - \chi_-^2)^{1/2}, \quad (8a)$$

$$\chi_\pm(k, \mathrm{Ro}) = \mathrm{Ro}^{-1} \pm \sqrt{k^2 + (\mathrm{Ro}^{-1}+1)^2}. \quad (8b)$$

Since $-1 < \epsilon < 1$, one can easily verify that $\mathrm{Re}(\sigma_-^{\pm}) = 0$ and $\mathrm{Re}(\sigma_+^-) \le 0$. Hence, the existence of an unstable horizontal mode is determined by $\mathrm{Re}(\sigma_+^+)$. The condition for horizontal instability (HI) is $|\chi_+| < |\epsilon|$. The vortex with given (Ro, ϵ) is unstable if this is satisfied for at least one value of k. The stability diagram is shown in Fig. 1. The *maximum* growth rate σ_m is

$$\sigma_m = \max_k \mathrm{Re}\left(\sqrt{\epsilon^2 - \chi_+^2}\right), \quad (9)$$

and the corresponding wave number $k = k_m$ is

$$k_m = \begin{cases} 0, & \mathrm{Ro} < -2, \\ \sqrt{-1 - 2\mathrm{Ro}^{-1}}, & -2 \le \mathrm{Ro} < 0. \end{cases} \quad (10)$$

Figure 2(a) shows σ_m, given by Eq. (9), as a function of (Ro, ϵ). Solid lines are contours of σ_m while dashed lines are contours of k_m given by Eq. (10).

In order to assess the role played by the magnetic field, in Fig. 2(b) we plot a similar diagram for the situation when the magnetic field is absent and the problem is reduced to that of the horizontal modes of elliptical instability with the Coriolis force, which had been studied before [17,21–25]. All Kelvin modes, regardless of their wavelength, now have the same growth rate $\sigma_0(\mathrm{Ro}, \epsilon)$ (solid lines), which is an eigenvalue of the matrix $\hat{S}_0(k)$ in the limit $k \to 0$,

$$\sigma_0 = \mathrm{Re}\left[\sqrt{\epsilon^2 - (1 + 2\,\mathrm{Ro}^{-1})^2}\right]. \quad (11)$$

The reason for this degeneracy is that the *unbounded flow* (2) has no intrinsic length scale. In the absence of magnetic field no unit of length is selected in any way [magnetic field

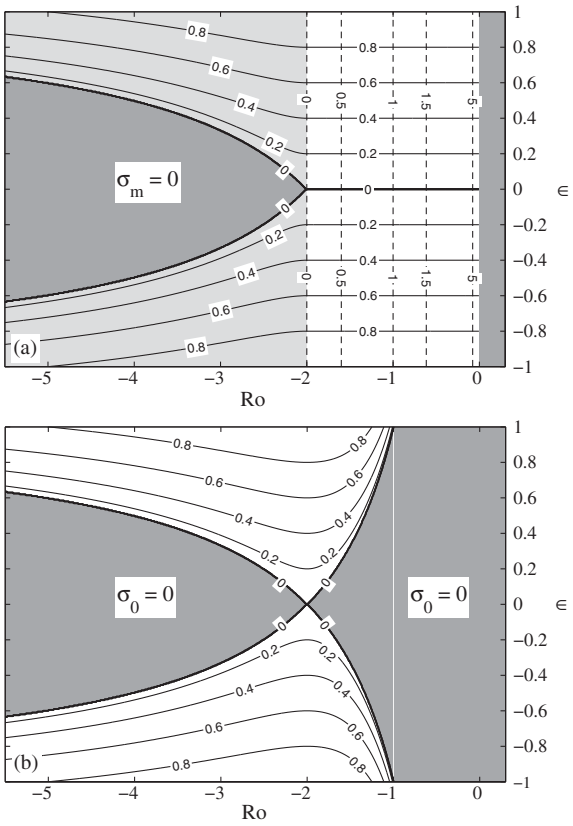

FIG. 2. Destabilizing effect of weak magnetic field. Shown are the level contours of the horizontal mode (HI) growth rate. Dark gray is the stable region in the (Ro, ϵ) parameter space. (a) Magnetic field present: Level contours of σ_m, given by Eq. (9) (solid lines), and of the wave number of the fastest growing mode k_m, given by Eq. (10) (dashed lines). Light gray is the region where $k_m = 0$; i.e., the fastest growing mode does not depend on z. For $-2 < \mathrm{Ro} < 0$ the fastest growing mode has finite wavelength ($k_m \neq 0$) and $k_m \to \infty$ as $\mathrm{Ro} \to 0^-$. (b) Magnetic field absent: Level contours of σ_0 given by Eq. (11) which is independent of k (all modes grow at equal rate). Dark gray stable region for $\mathrm{Ro} > -2$ disappears when the field is present.

introduces the length $u_A \gamma^{-1}$, cf. Eq. (3), and then the wavelength is measured in such units].

Important conclusions can now be drawn from Fig. 2.

(i) The instability of horizontal modes is *caused* by an *arbitrarily weak* magnetic field which, in the analysis, becomes an $O(1)$ quantity as soon as it is present. When $\mathrm{Ro} > -1$, it happens for any ϵ, and when $-2 < \mathrm{Ro} < -1$, it happens provided ϵ is not too large.

(ii) When the field is present, weak anticyclonic vortices ($-2 < \mathrm{Ro} < 0$) are *always* unstable to horizontal modes (provided $\epsilon \neq 0$). The more elliptical they are, the more violent the instability ($\sigma_m = |\epsilon|$). This is a short-wave instability with the wavelength decreasing to zero when $\mathrm{Ro} \to 0^-$ (in a dissipative fluid there would be a cutoff wavelength determined by viscosity [26] or by resistivity).

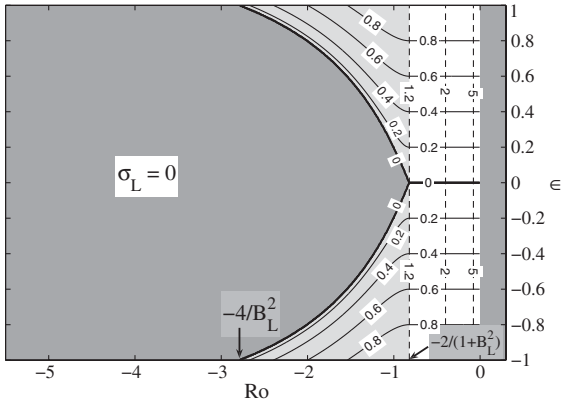

FIG. 3. Stability diagram for the HI modes in a bounded system with moderately strong magnetic field, $B_L = 1.2$. Plotted are level contours of the maximum growth rate σ_L (solid lines) and of the wave number of the fastest growing mode (dashed lines). Comparison with Fig. 2(a) indicates the stabilizing effect of strong magnetic field.

The physical explanation for the first conclusion is as follows. The nature of the $B \to 0$ limit is such that the *maximal growth rate* is independent of B. As B decreases, so does the wavelength of the fastest growing mode, but the growth rate remains the same for any $B \neq 0$. The simple reason is that the growth rate scales with ku_A. However small the Alfvén velocity (or B), sufficiently short wave will grow at finite rate. However, these modes do not exist when $B = 0$, so the $B \to 0$ limit is, in fact, singular (discontinuous).

Let us now consider the effect of finite-magnitude field, which cannot be regarded as weak. Since in an unbounded system the field magnitude can always be scaled out, as it enters the calculation only through the definition of units (3), there is then no distinction between weak and strong field (the only distinction is between "field present" and "field absent"). However, in a real system of finite size L [e.g., the depth of a planetary liquid core or, in our case, the thickness of the disk), the magnitude of the field can be characterized by the ratio of the two length scales, $B_L = (u_A \gamma^{-1})/L$]. We can then consider the effect of finite B_L and see that the modes destabilized by the weak field ($B_L \ll 1$) gradually become stable again when the field is strong ($B_L \gtrsim 1$). The reason is that in a bounded system there is an upper limit on the wavelength as a mode must "fit," i.e., $k^{-1}(u_A \gamma^{-1}) \lesssim L$ or $k \gtrsim B_L$. Calculating the maximum growth rate [see Eq. (9)], we now have to maximize over a restricted range of wave numbers, $k > B_L$, and thus obtain a smaller value $\sigma_L < \sigma_m$. The value of σ_L, as a function of Ro and ϵ, is plotted in Fig. 3. Comparing Figs. 2(a) and 3 shows the effect of finite B_L. When the field is (moderately) strong, $B_L = 1.2$, the stable region (dark gray) is much larger than in the weak-field (or large L) limit, in agreement with the intuition that (strong) field should be a stabilizing factor. For lower (more negative) values of Ro (i.e., $\mathrm{Ro} < -4/B_L^2$), the finite B_L effect, in

fact, eliminates all unstable HI modes. Importantly, for $\mathrm{Ro} > -2/(1+B_L^2)$ the modes have short wavelength and therefore remain unaffected.

We should stress that the notion of weak or strong field is meaningful only when some characteristic length scale L, independent of the field magnitude, can be identified in the system. The distance traveled by the Alfvén waves during one flow time unit (3) is then compared with that scale. Hence, the weak-field limit is equivalent to the large-L limit and vice versa, strong field'' means the same as ''compact system.''

We have shown that weak field acting on elliptical vortices (in a rotating frame) triggers some *particular modes* of instability (HI). The importance of this mechanism depends on whether these modes really dominate and thus determine the fate of the vortices. For Ro in the range $-2 < \mathrm{Ro} < -2/3$ and the field absent, there are no unstable linear modes of any kind [25], so the presence of the field really makes critical difference. Outside this range of Ro unstable resonant modes (not HI) do exist even in the absence of the magnetic field (see Ref. [27] for $\mathbf{\Omega} = 0$ and [16] for $\mathbf{\Omega} \neq 0$). Still, the field triggers the vigorous HI modes which can often be shown to dominate, i.e., to have faster growth rates, than the resonant modes. This can be shown analytically in the limit $\epsilon \to 0$ [16] and for $\epsilon \to 1$. Preliminary computations show this to be generally true for $-2/3 < \mathrm{Ro} < 0$, so we may expect that weak field really would decide the fate of the vortices in the right-hand gray patch in Fig. 2(b) and promote turbulent enhancement in them.

Astrophysical relevance of the HI modes and the results described above depends on whether (a) vortices are likely to have (Ro, ϵ) in the right-hand gray area of Fig. 2, and (b) the HI growth time scale is comparable with the vortex ''life expectancy'' (or shorter). When the vortex is created in a disk (with, say, $\Omega \sim r^n$), we may reasonably assume that its vorticity 2γ (calculated in the shearing box approximation [28,29], so relative to the frame comoving around the disk with the vortex center) is of the order of local ambient vorticity (i.e., shear) in the disk, $S = -r\partial\Omega/\partial r$. Suppose $2\gamma = -2S$ (vortex must be strong enough or shear will tear it apart). Then we obtain $\mathrm{Ro} = n$, so for a Keplerian disk we have $\mathrm{Ro} = -3/2$ and for galactic disk $\mathrm{Ro} = -1$, both values within the interesting range.

The value of ϵ can be estimated from the Kida model of the vortex patch in a shear flow [30], which gives $\mathrm{Ro} = n(1+\epsilon-\sqrt{1-\epsilon^2})^{-1}$. Hence, in the range $-2 < \mathrm{Ro} < -2/3$, most vulnerable to the HI modes, we obtain $0.6 < \epsilon < 1$ (Keplerian disk) and $0.4 < \epsilon < 0.9$ (galactic disk). Vortices vulnerable to unstable HI modes are therefore likely.

In the range $-2 < \mathrm{Ro} < -2/3$ the (dimensional) HI growth rate is $\sigma = \epsilon\gamma$ [cf. Fig. 2(a)]. The (dimensional) angular frequency of the vortex is $\omega = \sqrt{1-\epsilon^2}$. Hence, $\sigma/\omega > 0.7$ for Keplerian disks and $0.4 < \sigma/\omega < 2$ for galactic disks. In both cases the HI is clearly fast enough to affect even the short-lived vortices that survive only a few turn-over times.

One of us (K. B.) would like to thank Stéphane Le Dizès for helpful discussions. This work was supported by Polish Ministry for Science and Higher Education (Grant No. N307 022 32/0669), by the Interdisciplinary Centre for Mathematical and Computational Modelling (ICM), University of Warsaw (computational Grant No. G28-11), and by the COST Action MP0806.

*Also at: Interdisciplinary Center for Mathematical and Computer Modelling, University of Warsaw, Poland. On leave at Trinity College, Cambridge, UK. kbajer@fuw.edu.pl

†krzysztof.mizerski@gmail.com

[1] S. Chandrasekhar, Proc. R. Soc. A **216**, 293 (1953).
[2] R. J. Donnelly and M. Ozima, Phys. Rev. Lett. **4**, 497 (1960).
[3] E. P. Velikhov, Zh. Eksp. Teor. Fiz. **36**, 1398 (1959) [Sov. Phys. JETP **9**, 995 (1959)].
[4] S. Chandrasekhar, Proc. Natl. Acad. Sci. U.S.A. **46**, 253 (1960).
[5] S. A. Balbus and J. F. Hawley, Astrophys. J. **376**, 214 (1991).
[6] G. Rüdiger and R. Hollerbach, *The Magnetic Universe: Geophysical and Astrophysical Dynamo Theory* (Wiley, New York, 2004), 1st ed.
[7] R. T. Pierrehumbert, Phys. Rev. Lett. **57**, 2157 (1986).
[8] B. J. Bayly, Phys. Rev. Lett. **57**, 2160 (1986).
[9] J.-F. Donati, F. Paletou, J. Bouvier, and J. Ferreira, Nature (London) **438**, 466 (2005).
[10] J. M. Brown, G. A. Blake, C. Qi, C. P. Dullemond, D. J. Wilner, and J. P. Williams, Astrophys. J. **704**, 496 (2009).
[11] Z. Regály, A. Juhász, Z. Sándor, and C. P. Dullemond, Mon. Not. R. Astron. Soc. **419**, 1701 (2012).
[12] A. Bracco, P. H. Chavanis, A. Provenzale, and E. A. Spiegel, Phys. Fluids **11**, 2280 (1999).
[13] W. Lyra and H. Klahr, Astron. Astrophys. **527**, A138 (2011).
[14] A. Salhi and C. Cambon, Phys. Rev. E **79**, 036303 (2009).
[15] A. Salhi, T. Lehner, and C. Cambon, Phys. Rev. E **82**, 016315 (2010).
[16] K. A. Mizerski and K. Bajer, J. Fluid Mech. **632**, 401 (2009).
[17] T. Miyazaki, Phys. Fluids A **5**, 2702 (1993).
[18] H. K. Moffatt, in *Proceedings of the URSI—IUGG—International Colioquium on Atmospheric Turbulence and Radio Wave Propagation, Moscow, 1965*, edited by A. M. Yaglom and V. I. Tatarsky (Nauka, Moscow, 1967), pp. 139–154, http://moffatt.tc.
[19] C. Cambon, J.-P. Benoit, L. Shao, and L. Jacquin, J. Fluid Mech. **278**, 175 (1994).
[20] F. S. Godeferd, C. Cambon, and S. Leblanc, J. Fluid Mech. **449**, 1 (2001).

[21] A. D. D. Craik, J. Fluid Mech. **198**, 275 (1989).
[22] E. B. Gledzer and V. M. Ponomarev, J. Fluid Mech. **240**, 1 (1992).
[23] R. R. Kerswell, J. Fluid Mech. **274**, 219 (1994).
[24] S. Leblanc and C. Cambon, Phys. Fluids **9**, 1307 (1997).
[25] M. Le Bars, S. Le Dizès, and P. Le Gal, J. Fluid Mech. **585**, 323 (2007).
[26] S. Le Dizès, M. Rossi, and H. K. Moffatt, Phys. Fluids **8**, 2084 (1996).
[27] N. R. Lebovitz and E. Zweibel, Astrophys. J. **609**, 301 (2004).
[28] G. Lesur and J. C. B. Papaloizou, Astron. Astrophys. **498**, 1 (2009).
[29] K. A. Mizerski and W. Lyra, J. Fluid Mech. **698**, 358 (2012).
[30] S. Kida, J. Phys. Soc. Jpn. **50**, 3517 (1981).